Seasonal variability of crustal and marine trace elements in the aerosol at Neumayer Station, Antarctica

ROLF WELLER*[1], JANINA WÖLTJEN[1,2]; CLAUDIA PIEL[1], ROSA RESENBERG[1], DIETMAR WAGENBACH[3], GERT KÖNIG-LANGLO[1] and MICHAEL KRIEWS[1], *[1]Alfred Wegener Institute for Polar and Marine Research, Am Handelshafen 12, 27570 Bremerhaven, Germany, [2]Present address: School of Environmental Sciences, University of East Anglia, Norwich NR4 7TJ, UK, [3]Institut für Umweltphysik, University Heidelberg, Im Neuenheimer Feld 229, D-69120 Heidelberg, Germany*

* Correponding author.
e-mail: Rolf.Weller@awi.de

Version 30.04.2008

ABSTRACT

Atmospheric trace element concentrations were measured from March 1999 through December 2003 at the Air Chemistry Observatory of the German Antarctic station Neumayer by inductively coupled plasma – quadrupol mass spectrometry (ICP-QMS) and ion chromatography (IC). This continuous five year long record derived from weekly aerosol sampling revealed a distinct seasonal summer maximum for elements linked with mineral dust entry (Al, La, Ce, Nd) and a winter maximum for the mostly sea salt derived elements Li, Na, K, Mg, Ca, and Sr. The relative seasonal amplitude was around 1.7 and 1.4 for mineral dust (La) and sea salt aerosol (Na), respectively. On average a significant deviation regarding mean ocean water composition was apparent for Li, Mg, and Sr which could hardly be explained by mirabilite precipitation on freshly formed sea ice. In addition we observed all over the year a not clarified high variability of element ratios Li/Na, K/Na, Mg/Na, Ca/Na, and Sr/Na. We found an intriguing co-variation of Se concentrations with biogenic sulfur aerosols (methane sulfonate and non-sea salt sulfate), indicating a dominant marine biogenic source for this element linked with the marine biogenic sulfur source.

1. Introduction

The nearly completely ice covered Antarctic continent is virtually free of primary and secondary aerosol sources while the Southern Ocean is by far the dominant source to the Antarctic aerosol body making atmospheric sea salt and biogenic sulfur the major aerosol components (Wagenbach et al., 1998; Minikin et al., 1998). Terrestrial sources are limited to some insular rocky regions (on the Antarctic peninsula, in the coastal dry valleys and on high mountain ranges) and volcanic activity of Mt. Erebus. Nowadays, minor anthropogenic emissions arising from fossil fuel combustion during research and tourism activities may be considered as well. On the whole these natural and anthropogenic sources constitute local or regional trace element emissions of mineral dust, sulfur, and specific heavy metals which are thought to be of minor importance for the overall aerosol budget of Antarctica. Therefore, Antarctica offers an outstanding place to study the background composition and the natural biogeochemical cycling of aerosol.

Apart from ion analyses, only limited trace element measurements have been conducted so far in Antarctic aerosol samples as: at South Pole (Zoller et al., 1974; Cunningham and Zoller, 1981; Tuncel et al., 1989), at the Antarctic peninsula (Dick, 1991; Artaxo et al., 1992) and at coastal areas (i.e. Neumayer Station, Görlach, (1988) and Wagenbach et al. (1988)). In recent years the need for long term background aerosol studies, especially addressing the trace element composition, has been recognized. Certain heavy metals (e.g. Pb, Cd, Cr) can be employed as valuable tracers for the growing impact of anthropogenic heavy metal emissions for remote Antarctica (Wolff and Suttie, 1994; Wolff et al., 1999; Planchon et al., 2002). Furthermore, mineral dust derived trace elements like Fe may act as micronutrients affecting the biological activity of the ocean (Jickells et al., 2005), e.g. the atmospheric CO_2 burial (Bopp et al., 2003; Wolff et al., 2006) and the emission of dimethyl sulfide (DMS) (Turner et al., 2004), which is globally the most important precursor for natural sulfate aerosol. Finally,

mineral dust and sea salt profiles retrieved from polar ice cores have proven to provide a wealth of paleoclimatic information (e.g. Petit et al., 1999; Wolff et al., 2006; Fischer et al., 2007; Ruth et al., 2007). For improving the interpretation of these records, a better knowledge about long range transported continental dust and regional derived sea salt would be needed, especially including the seasonality of their atmospheric loading and entry into the Antarctic continent. Concerning sea salt aerosol, the formation on freshly formed sea ice, associated with a significant sea salt fractionation, has been put forward as an alternative source (Rankin et al., 2000 and 2002; Wolff et al., 2003) to the accepted process by wind induced bubble bursting over open ocean water (Monahan et al., 1986). If the significance of this source proves true, it would entail a paradigm shift in the interpretation of sea salt profiles from polar ice cores (Wolff et al., 2003).

Here, we present atmospheric trace element records mainly associated with mineral dust and marine sources which are continuously observed between 1999-2003 at the German Antarctic Neumayer Station. Primarily focusing on seasonal aspects, the weekly filter samples were analysed by ICP-QMS for the trace element Li, Na, K, Mg, Ca, Sr, Al, La, Ce, Nd, and Se. The ICP-QMS results are supported by our regular IC analyses providing complementary information on the ionic aerosol composition with respect to methane sulfonate, sulfate, Na^+, NH_4^+, K^+, Mg^{2+}, and Ca^{2+}.

2. Methods

2.1. Measurement Site and Meteorological Conditions

Aerosol sampling was made at the Air Chemistry Observatory, about 1.5 km south of Neumayer station (70^o 39' S, 8^o 15'W). During the summer months, the bay and the nearby ice edge are mainly free of sea ice and there is always open water present. Apart from a few nunataks about 100 km south of the station there are no ice-free land surfaces near Neumayer,

and the probability of contact with air masses from ice-free continents is small. In general there are two different wind regimes: (1) Strong synoptically affected winds are from the East with infrequent geostrophically intensified switches to the West and (2) weak katabatic winds from southern directions. The air mass transport pattern to Neumayer Station was investigated by Kottmeier and Fay (1998) and a more detailed picture on the climatology at Neumayer Station can be found in König-Langlo et al. (1998).

Aerosol was collected on Whatman 541 cellulose filters which were precleaned by soaking in HCl followed by rinsing with de-ionize water until virtually no enhancement of the electrolytical conductivity could be detected. The aerosol was continuously sampled at 120 m^3 h^{-1} by two filters (diameter 240 mm) in series using a ventilated electropolished stainless steel inlet stack (total height about 8 m above the snow surface) with a 50% aerodynamic cut-off diameter around 7-10 µm at wind velocities between 4-10 m s^{-1}. This high volume sampling technique is part of the continuous long-term observation programme carried out since 1983 at Neumayer. Here we refer to samples taken from March 1999 through December 2003. These data were based on a sampling period of typically 7 days which corresponds to a probe volume of around $2x10^4$ m^3 STP. A more detailed description of the sampling procedure itself is given in Wagenbach et al. (1988).

Local pollution by vehicles and the base itself is a potential problem for many measurements concerning the background status of the Antarctic troposphere. To ensure contamination free air sampling, the Air Chemistry Observatory is situated in a clean air facility approximately 1.5 km south of Neumayer. Due to the fact that northerly wind directions are very rare, contamination from the base can be excluded for most of the time. Additionally, the power supply (20 kW) is provided by cable from the main station, thus no fuel driven generator is operated in the observatory vicinity. Finally, contamination-free sampling is controlled by the permanently recorded wind velocity, wind direction and by the condensation particle

(CP) concentration. Contamination was indicated for each of the following criteria: Wind direction within a 330°-30° sector, wind velocity <2.0 m s^{-1} and/or CP concentrations (measured by a TSI CPC 3022A particle counter) >2500 cm^{-3} during summer, >800 cm^{-3} during spring/autumn and >400 cm^{-3} during winter. The CP threshold values were chosen based on our more than 20-year long CP record from Neumayer, demonstrating that CP concentrations above the corresponding levels can usually be traced back to local pollution. In case of contamination, given by these criteria, an automatic interrupt of the sampling procedure was initiated within one second (shut down of the pumps and closing the electromotive valves typically needed around 10 seconds). Sampling was restarted after recurrence of clean air conditions and a delay of two minutes. However, most of the data loss was provoked by blizzards and drifting snow (wind velocity >20 m s^{-1}). During such harsh weather conditions aerosol sampling has to be switched off (due to the danger of snow entering the inlet) which entailed a downtime of roughly 10% of the observation period. Note, that <2% of data loss was actually caused by potential contamination.

2.2. Analytical Methods

2.2.1. ICP-QMS Analysis

Trace element analysis was performed by means of ICP-QMS (ELAN 6000, Sciex/Perkin Elmer) equipped with a cross-flow nebulizer as sample introduction system. The alignment of the instrument (plasma torch, ion lens, gas flow, nebulizer) was checked and adjusted before analysis by daily performance solutions containing a mixture of 10 ng g^{-1} Mg, Ba, Ce, Pb, and Rh. One half of each filter was used for trace element analysis, while another 1/6 of each filter was used for IC analysis (see below). For trace element analyses we chose a total digestion of the samples in order to quantitatively dissolve all mineral compounds, which is not been given by simple acidic (HNO_3) leaching (Lindberg and Harris, 1983; Reinhardt et al., 2003,

169 Table 5 therein). Thus these aliquots were subject to a pressurized digestion system (DAS
170 100, Picotrace) at 200°C in a mixture containing HNO_3 (suprapure, 65%, Merck, sub-boiling
171 bi-distilled), HF (suprapure, 40%, Merck, sub-boiling bi-distilled) and H_2O_2 (suprapure, 30%,
172 Merck). With this device a series of 24 samples could be digested in parallel. Each series
173 included one filter blank and a certified reference sample (NIST 1648 urban particulate mat-
174 ter). For calibration we used commercially available standard solutions (10^4 ppb multielement
175 verification standard 1 and 2, Perkin Elmer) which were generally applied in 1 ppb, 10 ppb,
176 and 100 ppb concentrations (1 ppb corresponds to 1 ng of each element in 1 g solute). Each
177 sample was spiked by 10 ppb Rh as internal standard to normalize the signal intensities and
178 compensate instrumental sensitivity variations. The instrumental detection limits (IDL) were
179 derived from 60 blank solutions and correspond to three times the standard deviation (std) of
180 these blank values (Table 1). Based on the results of the NIST reference material, the retrieval
181 for each element to be discussed here was generally between 95% and 100%. When analysing
182 the filter samples of the years 2002 and 2003 we were frequently faced with abnormally
183 elevated Al-blanks prohibiting further evaluation. Thus the time series of this period appeared
184 fragmentary. Due to these unexplained analytical problem, we decided to use the consistently
185 measured La as mineral dust tracer and reference element for calculating crustal enrichment
186 factors.

187 The variability of the filter procedure blanks clearly governed the overall accuracy as well
188 as the analytical detection limits. These estimates were derived from the variation of 49 iden-
189 tically processed procedure blanks and include possible contributions by the previously
190 cleaned filters and any effects arising from handling and storage. We conservatively estimated
191 the method detection limits (MDL) as three times the standard deviation (std) of these overall
192 blank values (Table 1). In addition to this blank induced uncertainty, relative ICP-QMS cali-
193 bration errors were considered. In short, the combined uncertainty was found to be approxi-

194 mately between ±8% and ±12% for element concentrations above three times the correspond-
195 ing MDL. It increased from around ±(15-20)% approaching 3xMDL level to roughly (+50/-
196 100)% close to the MDL. The final atmospheric concentrations (in ng m^{-3} or pg m^{-3}) were
197 calculated from the blank corrected element amounts and the corrected sampled air volume to
198 standard conditions (273.16 K and 1013 hPa).
199
200 **2.2.2. IC Analysis**
201 The extraction of the aliquots for IC analysis included soaking and shaking in 50 ml MilliQ
202 water, followed by ultrasonic treatment for 15 minutes. All samples were analyzed for meth-
203 ane sulfonate (MS), Cl^-, Br^-, NO_3^-, SO_4^{2-}, Na^+, NH_4^+, K^+, Mg^{2+}, and Ca^{2+} by IC analysis. For
204 details concerning IC set up, the determination of accuracy and detection limits see Piel
205 (2004). Errors were determined from the blank variability, the typical IC error (calibration
206 error and baseline noise), and the error from the sample air volume. In short, the combined
207 uncertainty was between ±5% and ±11% for the components MS, Cl^-, NO_3^-, SO_4^{2-}, Na^+, K^+,
208 Mg^{2+}, and Ca^{2+} and approximately ±27% for species Br^- and NH_4^+. Non-sea salt sulfate (nss-
209 SO_4^{2-}) concentrations were calculated by subtracting the concentration of the sea salt derived
210 sulfate from the total SO_4^{2-} concentration (in ng g^{-1}). We used Na^+ as sea salt reference spe-
211 cies and the sulfate to sodium ratio in bulk sea water of 0.252 for November to February, and
212 due to the potential impact of sea salt fractionation by frost flower formation a factor of 0.07
213 for winter (March – October) samples (Wagenbach et al., 1998). Note that with our sampling
214 technique, gaseous HCl, HBr, HNO_3, and NH_3 were partly collected on the filter material and
215 contributed to the reported Cl^-, Br^-, NO_3^-, and NH_4^+ concentrations.
216 For the elements Na, K, Mg, and Ca an inter-comparison with the corresponding concentra-
217 tions measured by IC was possible. A reduced major axis regression (RMA) revealed a good
218 agreement between ICP-QMS and IC for Na and Mg, while the ICP-QMS systematically

219 provided higher K and lower Ca concentrations (Table 2). For these two elements the results
220 from the IC-analytics were used throughout the paper because they appeared more reliable.
221 Apart from known problems associated with the detection of K and Ca by ICP-QMS (mainly
222 interferences from Ar carrier gas of the plasma), a possible explanation in case of Ca may be
223 the formation of hardly soluble CaF_2 during digestion. The relatively high scatter of the data
224 around the regression line, expressed by somewhat low regression coefficients r^2 (Table 2),
225 may partly be due to the fact that ICP-QMS and IC analyses were performed with different
226 aliquots of the corresponding filters.
227
228

229 # 3. Results and Discussion

230 ## 3.1. Classification of Trace Elements

231 We first calculated for each element M the so-called crustal EF_{crust} and sea salt EF_{ss} enrich-
232 ment factors, respectively as:

233 $$EF_{crust} = \frac{(M/La)_{aerosol}}{(M/La)_{crust}}, \qquad EF_{ss} = \frac{(M/Na)_{aerosol}}{(M/Na)_{ss}}$$

234 For reasons discussed in the analytical section, we chose as marker for mineral dust La and
235 refer to the crustal composition reported in Wedepohl (1995). Note that at Neumayer Ca is
236 largely sea salt derived (see below) and thus an unfavourable tracer for mineral dust. For the
237 corresponding EF_{ss} we rely on standard mean ocean composition reported in Holland (1993).
238 In Fig. 1 the results are presented for winter and summer. Because the ocean is well mixed,
239 even small deviations from the standard mean ocean composition indicate that either the
240 given component was only partially associated with sea salt or a sea salt fractionation during
241 aerosol formation/transport occurred. The situation is intrinsically much more complicated in
242 case of mineral dust. First of all the crustal composition of the earth exhibits a pronounced

variability (Wedepohl, 1995). Apart from this, weathering and mineral dust generating processes usually entail a distinct fractionation. Also the crustal element composition may significantly differ between mean crust, soil and the small (clay) particles being readily long range transported. Here, we conservatively assume that EF_{crust} values above 10 point at a negligible mineral dust source. The enrichment factors indicate crustal material as the main source for the elements Al, Nd, and Ce, while, on the other hand, Li, K, Mg, Ca, and Sr were primarily sea salt derived elements, though this dissection appears equivocal for Li. Selenium in contrast was found to be highly enriched relative to crust, but also with respect to (sea salt) Na pointing to anthropogenic or biogenic sources.

3.2. Overview on the Trace Element Concentrations measured at Neumayer Station

Table 3 gives a compendium of the trace element concentrations measured five years at Neumayer Station. In addition individual time series of trace elements representative for sea salt aerosol (Li, Na, Sr) and mineral dust (Al, La, Ce, Nd) species are presented in Figures 2 and 3. Generally, trace element concentrations at Neumayer exhibited a striking inter-annual and seasonal variability. Apart from the general sparseness of data available from other Antarctic sites, the intrinsic strong variability makes a coherent assessment of the inter-site differences a difficult task. Especially the extraordinarily high atmospheric Se and Al levels reported by Artaxo et al. (1992) remain unexplained (Table 4).

Görlach (1988) used acid extractable Mn and Wagenbach (1996) combined Mn and Al as mineral dust proxy at Neumayer. Converting the reported Mn from Görlach (1988) into corresponding La concentrations (using a mean crust composition given in Wedepohl (1995), i.e. Mn/La = 23.9) resulted in a summer maximum of around 1.1 pg m^{-3} and a winter minimum of 0.21 pg m^{-3}. This is systematically lower (by 0.21 pg m^{-3} and 0.35 pg m^{-3}, respectively) but still in fair agreement with our La results (Table 3). A pronounced seasonal Al (i.e. mineral

dust) maximum during austral summer was evident at all sites, with a mineral dust entry tentatively higher at coastal Neumayer compared to continental South Pole (Table 4). The data from the Antarctic Peninsula tip appeared contradicting, and the mentioned outstanding high Al values reported by Artaxo et al. (1992) might most probably be caused by sporadic local dust production from the rocky adjacencies. In contrast to the observed marginal gradient from coastal to continental Antarctica for mineral dust related trace elements, Na (i.e. sea salt) concentrations were about an order of magnitude higher at coastal sites.

3.3. Seasonal Aspects

3.3.1. Synopsis of the seasonality of the aerosol budget at Neumayer

In order to assess the relative composition of the aerosol (by mass) and its seasonality, we included the relevant ionic compounds. Therefore we considered the aerosol compounds sea salt (calculated from the measured Na) mineral dust (calculated from the measured La) and further MS, nss-SO_4^{2-}, Cl^-, NO_3^-, and NH_4^+ from the IC analyses. Clearly, the aerosol at Neumayer was dominated by sea salt particles (Fig. 4), even during summer when biogenic sulfur emissions reach their distinct annual maximum (Minikin et al., 1998), while mineral dust was generally a minor compound with a maximum mass fraction of about 5% during summer. Figure 5 shows in more detail the annual cycle of the compounds sea salt, mineral dust and biogenic sulfur (sum of MS and nss-SO_4^{2-}). In terms of aerosol composition (biogenic, sea salt, and mineral dust) the polar winter seemed confined between April and end October with the turn of the seasons occurring in March/April and October/November.

3.3.2. Seasonality of mineral dust and sea salt entry at Neumayer

Figures 2 and 3 indicate that mineral dust and sea salt derived trace elements (Al, La, Ce, Nd, and Li, Na, K, Mg, Ca, Sr, respectively) were characterized by distinct mean annual

cycles. In Figure 6 the mean seasonal cycle of the crustal and sea salt reference are displayed in monthly concentrations (± standard deviation). The seasonality was most pronounced for the crustal elements with a distinct concentration maximum from October through March, while for sea salt aerosol a broad maximum between April and September was evident. The mean relative seasonal amplitude, i.e. the mean maximum normalized to the corresponding annual mean, was around 1.7 and 1.4 for mineral dust (La) and sea salt aerosol (Na), respectively. In addition, enrichment factors also exhibited a distinct seasonality, with higher EF_{crust} but lower EF_{ss} in winter and vice versa (Figure 1). A possible reason for this finding might be the seasonality of dust and sea salt entry observed at Neumayer. During the seasonal maximum of atmospheric dust entry in summer and sea salt concentrations in winter, the corresponding enrichment factors were lowest due to the dilution of a given enrichment effect by enhanced crustal dust or sea salt material, repectively.

The observed seasonality for mineral dust appeared consistent with previous studies from Neumayer (Görlach, 1988; Wagenbach et al., 1988, Wagenbach, 1996), as well as South Pole (Cunningham and Zoller, 1981; Tuncel et al., 1989), where Mn and Al was used as tracer for mineral dust, respectively. A thorough evaluation of sea salt aerosol concentrations measured at various coastal stations was given in Wagenbach et al. (1998). In agreement with our findings, these authors reported a broad Na maximum during winter at Neumayer, which has also been observed at South Pole (Tuncel et al., 1989). In general, an annual cycle of aerosol components observed at remote, source free sites can be attributed to a combination in the seasonality of the source strength and atmospheric transport processes. While for sea salt aerosol regional or even local sources have to be considered, the source regions for mineral dust on the surrounding continents are more than 4000 km away and consequently long range transport, most probably via the free troposphere, is decisive (Genthon, 1992; Krinner and Genthon, 2003). It is believed that the main provenances for Antarctic mineral dust are the

Patagonian loess regions (Smith et al., 2003). The seasonal contrast of Patagonian dust fluxes seems by far not as distinct as those of the atmospheric rare earth element (equivalent to mineral dust) concentrations at Neumayer, though a broad maximum between October and March is discernible (Gaiero et al., 2003, Figure 14 therein). In addition to this somewhat ambiguous source strength seasonality, we may expect a clear annual cycle in the atmospheric mixing height above continents (typically maximum during summer). Since long range dust transport to Antarctica is favoured via the mid troposphere, a more effective transfer of dusty boundary layer into high altitudes during the summer half year would be consistent with a Neumayer summer maximum as well. This explanation is supported by measurements of a basically similar seasonality seen at this site for the long lived ^{222}Rn decay product ^{210}Pb (Wagenbach et al., 1988), known to have a rather constant (continental) emission rate and to be less effectively washed out than the typically coarse mode mineral dust particles. Therefore the observed mineral dust maximum at Neumayer is probably a combined result of the seasonality in dust generation and the more efficient uplift of dust loaded air into the free troposphere in summer.

The most efficient global mechanism producing sea salt aerosol is bubble bursting during whitecap formation and dispersion of wave crests by surface winds over open ocean waters (Monahan et al., 1986). Thus, sea salt production exhibits a strong dependency on wind speed (Fitzgerald, 1991). Compatible with this perception is the fact that storminess and wind velocity exhibit a broad maximum during the winter months at Neumayer (Fig. 7). However, as for the individual data points there was virtually no correlation between wind velocity and observed Na concentrations ($r^2 = 0.07$). Note that this was also true for our low volume aerosol samples taken at daily resolution between October 2003 and February 2007 (teflon-nylon filter combinations, analysed by IC). It seems that the general weather situation over the South Atlantic was decisive and the most efficient sea salt production occurred during passing

cyclones (Wyputta, 1997). However, the sea salt aerosol loading at Neumayer should also depend on the efficiency of the transport process, removal by wet deposition, and the actual sea-ice cover. The interplay of these factors may have blurred a simple correlation with the local wind speed. In this regard, however, we have to bear in mind that particles above an aerodynamic diameter of around 7-10 µm, which may constitute a significant if not dominant fraction of the sea salt aerosol mass from nearby sources, were not adequately sampled due to the cut-off of our air inlet.

The formation of sea salt aerosols by frost flowers and associated processes suggested by Wolff et al. (2003) should be most active between March and September, consistent with the observed Na seasonality. Again it can be assumed that high wind velocities are still necessary to finally create sea salt aerosols by dispersion and mobilisation of frost flowers, a process which is actually not yet clarified.

3.3.4. Sea salt fractionation

There is some evidence that during wind induced sea salt aerosol generation over open ocean waters, a fractionation of major ions (Na^+, Mg^{2+}, K^+, Cl^-, and SO_4^{2-}) relative to bulk seawater is negligible, except for Ca^{2+} which appeared significantly enriched (Keene et al., 2007). On the other hand, sea ice formation entails considerable sea salt fractionation which could influence sea salt aerosol composition if freshly formed sea ice acts as a significant source. Below -6.3°C solid $Na_2SO_4 \cdot 10H_2O$ (mirabilite) crystallizes, followed by $CaSO_4 \cdot 2H_2O$ (gypsum), and $NaCl \cdot 2H_2O$ (hydrohalite) precipitation at -22.2°C and -22.9°C, respectively (Marion and Farren, 1999). A complete mirabilite precipitation, probably the dominant fractionation process on freshly formed sea ice, would lead to a Na depletion of about 11.8% by mass. Assuming simply that no fractionation would occur for the sea salt compounds Li, K, Mg, and Sr, a corresponding increase of the enrichment factors EF_{ss} to around 1.12 should be

368 expected in sea salt aerosol for this species during winter when sea salt fractionation is most
369 probable. In fact, Rankin et al. (2000) found Mg and Ca enrichment factors in frost flower
370 samples near Halley Station (EF_{ss}(Mg) = 1.16, and EF_{ss}(Ca) = 1.15), roughly compatible with
371 mirabilite precipitation but indicating, if at all, a negligible gypsum precipitation. Also analy-
372 ses of individual aerosol particles sampled at the coastal Syowa Station evidenced fraction-
373 ated Mg-rich (and Ca-rich) sea salt particles (Hara et al., 2005).

374 Combining our ICP-QMS and IC results allows to determine sea salt fractionation for an
375 extended number of sea-salt related trace elements. In our approach we first corrected Li, K,
376 Mg, Ca, and Sr concentrations for the minor crustal contribution (which were generally be-
377 tween 1% and 8%) to derive enrichment factors EF_{ss}(ssM) exclusively for the sea salt portion
378 of these elements. To be consistent, we generally referred ssK and ssCa values to ssNa all
379 taken from IC analyses, while for the other elements (Li, Mg, Sr) we relied on the ICP-QMS
380 results and related them to ssNa also determined by ICP-QMS. In this way we circumvent
381 potential discrepancies caused by systematic analytical differences of both methods (see
382 section 2.2.2).

383 All Na_{ss} based EF_{ss}(ssM) values were strikingly variable throughout the year and, except
384 Ca, did not exhibit a significant seasonality as would have to be expected from a depleted
385 ssNa reference during winter (Figure 8). It is important to note that in terms of analytical
386 accuracy departures beyond ±20% (in the worst case, at very low concentrations, beyond
387 ±50%) from standard mean ocean water (SMOW) should be regarded as significant. Another,
388 but hardly conceivable reason for the scatter of EF_{ss}(ssM) could be more than an order of
389 magnitude higher crustal M/La ratios (M = Li, Na, K, Mg, Ca, Sr) than reported by Wedepohl
390 (1995), which would strongly increase the crustal corrections and thus the uncertainty of the
391 calculated ratios. Concerning the medium departures of EF_{ss}(ssM) from SMOW, Figure 8
392 reveals that ssLi and ssMg were enriched by a factor 2.2 and 1.2, respectively, while ssSr was

393 depleted throughout (EF_{ss}(ssSr) = 0.72). For ssK and ssCa the (median) deviation from
394 SMOW was not significant, except for the winter values of ssCa ($EF_{ss}(ssCa)_{winter}$ = 1.34). In
395 double-logarithmic plots of ssM (M = Li, K, Mg, Ca, Sr) versus the ssNa reference it becomes
396 apparent that departures from SMOW occurred equally over the whole measured concentra-
397 tion range and that for ssLi, ssMg, and ssSr the data points were displaced from the SMOW-
398 line (Fig. 9). Obviously, the high variability of EF_{ss}(ssM) in general, as well as the median
399 departures from SMOW for ssLi and ssSr cannot be explained by mirabilite precipitation
400 alone. Finally the scatter of the enrichment factors (Figures 8 and 9) were strikingly higher
401 than the results from recent laboratory investigations on sea salt aerosol formation over a
402 realistic air/sea interface (Keene et al., 2007). In summary, our results suggest that in the
403 present case additional unknown fractionation processes occurred during sea salt aerosol
404 production over the whole year at the interface air/sea or air/sea-ice or subsequently during
405 atmospheric transport and sampling.
406
407 **3.3.4. Source and seasonality of atmospheric Se**
408 It is believed that natural sources like sea spray, volcanoes, and the biosphere dominate the
409 global budget of atmospheric Se by around 60%, while the remaining anthropogenic sources
410 (basically fossil fuel combustion and mining) are mainly concentrated in the northern hemi-
411 sphere (Mosher and Duce, 1987). As noted by Mosher (1986), the natural and anthropogenic
412 Se cycles are closely linked through the biosphere. The distinct seasonal Se concentration
413 maximum during summer observed at Neumayer suggests a potential biogenic source.
414 Amouroux et al., (2001) have demonstrated that the production of gaseous selenium species
415 coincided with phytoplankton blooms responsible for dimethyl sulfide (DMS) emission. It
416 was found, that the sulfur atom in DMS can be substituted by selenium (Mosher et al., 1987;
417 Amouroux et al., 2001). Consequently, atmospheric Se should be closely coupled to the DMS

turnover. In fact we observed a significant correlation between Se and the end products of photochemical DMS oxidation, MS and nss-SO_4^{2-} (r(MS) = 0.66; r(nss-SO_4^{2-}) = 0.67). The co-variation of Se and MS time series is shown in Fig. 10. Even the inter-annual variability largely coincided. Atmospheric Se concentrations found at South Pole were significantly lower (Table 4) but showed the same seasonality with maximum values of 8.4±1.6 pg m^{-3} during summer (winter concentration: 4.8±0.8 pg m^{-3} (Tuncel et al., 1989)), in accordance with a prominent marine biogenic source which should be less discernible in continental Antarctica.

Apart from this overall consistent picture there remain several open questions. First of all, we have to consider that the sampling efficiency of total Se is not well specified. Inspecting some of our Whatman 541 back-up filter showed no Se concentrations above the typical blank value, in agreement with results by Mosher et al. (1987) who used Whatman 41 filters. In contrast, Mosher (1986) reported on low sampling efficiencies (65%-45%) for this filter type in his thesis. Apart from this, knowledge on speciation of atmospheric Se is poor. Apparently, DMSe, elemental Se, as well as SeO_2 can be chemically transformed into water soluble selenite (SeO_3^{2-}) and selenate (SeO_4^{2-}) in the atmosphere (Wen and Carignan, 2007). In marine environments an enrichment of Se-compounds in sub-micron aerosol particles (mainly sea salt particles) was suggested (Wen and Carignan, 2007). It is not clarified to what extend volatile organic and inorganic Se species (e.g. DMSe, Se, SeO_2) are retained and likely chemically transformed on the used filter material during the typical sampling interval of 7 days. Another issue are considerable Se background concentrations measured during polar night (at Neumayer and South Pole) when regional biogenic activity ceases. This is in contrast to negligible MS concentrations generally observed during winter (Figure 10). Hence we tentatively assign wintertime atmospheric Se levels at Neumayer mainly to the global background load of Se. According to Cunningham and Zoller (1981), the atmospheric load of

443 volatile elements like As and Se at South Pole could also be influenced by volcanic emissions.
444 These authors ascribed a distinct Se peak in their time series to the explosive eruption of
445 Ngauruhoe volcano in New Zealand that happened in 1975. In our case, however, the contri-
446 bution of volcanic Se emissions should be, if at all, of minor importance due to the distance of
447 the sole presently active but calm volcanoes Mt. Erebus and Mt. Melbourne. Above all, the
448 observed seasonality of the Se signal at Neumayer can hardly be explained by volcanic impact
449 but might partly be responsible for background Se concentrations. Interestingly, wintertime
450 Se levels at Neumayer were about a factor of three higher compared to South Pole, where the
451 impact of Mt. Erebus should be more pronounced. For mineral dust derived trace elements
452 (Al, La) a similar but weaker gradient is apparent (Table 4), suggesting that the more pro-
453 nounced and deeper stable inversion layer at South Pole hampers down mixing of long range
454 transported trace compounds. In addition further minor, yet unexplained Se sources (local
455 contamination, still active regional biogenic emissions) possibly have to be considered at
456 Neumayer.
457
458

459 ## 5. Conclusion

460 In contrast to the ionic composition of Antarctic aerosol, corresponding continuous long
461 term observations of atmospheric trace element concentrations are so far restricted to South
462 Pole and Neumayer. Even from these sites, complete year round data records do not cover
463 more than 5 years in series. Our results revealed a distinct and contrary seasonality of mineral
464 dust and sea salt load at Neumayer which, along with previous results, seems to be valid for
465 coastal as well as continental Antarctica. At coastal sites, mineral dust load appeared some-
466 what more pronounced. More observations from different sites are necessary to establish a
467 potential difference between continental and coastal Antarctica in trace element entry. Pro-

vided that mineral dust is widely uniformly distributed in the free troposphere above Antarctica, this could give us some information on the role of the stable inversion layer, which is most pronounced in continental Antarctica, as a barrier against air mass down mixing. This would be especially interesting to scrutinize and constrain models addressing aerosol deposition in Antarctica. Another interesting point was the striking variability of the measured ssM/ssNa ratios for M = Li, K, Mg, Ca, and Sr, suggesting that apart from sea salt formation in sea ice covered regions itself, sea salt aerosol fractionation processes are not sufficiently clarified. As a consequence we are still lacking a tracer to reliably assess sea salt production on sea ice, a crucial point for the interpretation of sea salt records in polar ice cores. Marine biochemistry was most probably the dominant source for Se. An interesting open question is, how much Se is persistently deposited in polar snow and may serve as a proxy for biogenic activity in polar ice cores. Clearly, more investigations on the atmospheric photochemistry of marine biogenic selenium as well as the chemical nature of particulate atmospheric Se are required.

Acknowledgements. The authors would like to thank the technicians and scientists of the Neumayer overwintering crews of the years 1999-2003. Helpful comments and suggestions on the manuscript by an anonymous reviewer is greatly appreciated. This is AWI publication no. xy. Data are available from Pangaea (doi:10.1594/PANGAEA.691456).

References

Amouroux, D., Liss, P.S., Tessier, E., Hamren-Larsson, M., and Donard, O.F.X. 2001. Role of oceans as biogenic sources of selenium. *Earth Planet. Sci. Lett.* **189**, 277-283.

Artaxo, P., Rabello, M.L.C., Maenhaut, W., and van Grieken, R. 1992. Trace elements and individual particle analyis of atmospheric aerosols from the Antrctic peninsula. *Tellus* **44B**, 318-334.

Bopp, L., Kohfeld, K.E., Le Quéré, C., Aumont, O. 2003. Dust impact on marine biota and atmospheric CO_2 during glacial periods. *Paleoceanography* **18**(2), doi:10.1029/2002PA000810.

Cunningham, W.C. and Zoller, W.H. 1981. The chemical composition of remote area aerosols. *J. Aerosol Sci.,* **12**(4), 367-384.

Dick, A.L. 1991. Concentrations and sources of metals in the Antarctic Peninsula aerosol. *Geochim. Cosmochim. Acta*, **55**, 1827-1836.

Fischer, H., Siggaard-Andersen, M.-L., Ruth, U., Röthlisberger, R., and Wolff, E. 2007. Glacial/interglacial changes in mineral dust and sea-salt records in polar ice cores: sources, transport, and deposition. *Rev. Geophys.* **45**, RG1002, doi:10.1029/2005RG000192.

Fitzgerald, J.W. 1991. Marine aerosols: A review. *Atmos. Environ. Part A*, **25**, 533-546.

Gaiero, D.M., Probst, J.-L., Depetris, P.J., Bidart, S.M., and Leleyter, L. 2003. Iron and other metals in Patagonian riverborne and windborne materials: Geochemical control and transport to the southern South Atlantic Ocean. *Geochim. Cosmochim. Acta* **67**(19), 3603-3623.

Genthon, C. 1992. Simulations of desert dust and sea-salt aerosol in Antarctica with a general circulation model of the atmosphere. *Tellus* **44B**, 371-389.

510 Görlach, U. 1988. Die jahreszeitliche Variation von atmosphärischem Blei, Zink und Mangan
511 im antarktischen Küstenbereich, PhD-Thesis. Ruprecht-Karls-Universität Heidelberg, Hei-
512 delberg.
513 Hara, K., Osada, K., Kido, M., Matsunaga, K., Iwasaka, Y., Hashida, G., and Yamanouchi, T.
514 2005. Variations of constituents of individual sea-salt particles at Syowa station, Antarc-
515 tica. *Tellus* **57B**, 230-246.
516 Holland, H.D. 1993. The chemistry of atmosphere and oceans, John Wiley & Sons, 1. edition,
517 New York, 154-157.
518 Jickells, T.D., An, Z.S., Andersen, K.K., Baker, A.R., Bergametti, G., and co-authors. 2005.
519 Global Iron Connections Between Desert Dust, Ocean Biogeochemistry, and Climate. *Sci-*
520 *ence* **308**, 67-71, doi:10.1126/science.1105959.
521 Keene, W.C., Maring, H., Maben, J., Kieber, D.J., Pszenny, A.A.P. and co-authors. 2007.
522 Chemical and physical characteristics of nascent aerosol produced by bursting bubbles at a
523 model air-sea interface. *J. Geophys. Res.*, **112**, D21202, doi:10.1029/2007/JD008464.
524 König-Langlo, G., King, J.C., Pettré, P. 1998. Climatology of the three coastal Antarctic
525 stations Dumont d'Urville, Neumayer and Halley. *J. Geophys. Res.* **103**(D9), 10 935-10
526 946.
527 Kottmeier, C. and Fay, B. 1998. Trajectories in the Antarctic lower troposphere. *J. Geophys.*
528 *Res.* **103,** 10 947-10 959.
529 Krinner, G. and Genthon, C. 2003. Tropospheric transport of continental tracers towards
530 Antarctica under varying climatic conditions. *Tellus* **55B**, 54-70.
531 Lindberg, S.E. and Harris, R.C. 1983. Water and acid soluble trace metals in atmospheric
532 particles. *J. Geophys. Res.* **88**(C9), 5091-5100.

533 Marion, G.M. and Farren, R.E. 1999. Mineral solubilities in the Na-K-Mg-Ca-Cl-SO_4-H_2O
534 system: A re-evaluation of the sulfate chemistry in the Spencer-Møller-Weare model. *Geo-*
535 *chim. Cosmochim. Acta*, **63**, No. 9, 1305-1318.
536 Minikin, A., Legrand, M., Hall, J., Wagenbach, D., Kleefeld, C., Wolff, E., Pasteur, E.C., and
537 Ducroz, F. 1998. Sulfur-containing species (sulfate and methanesulfonate) in coastal Ant-
538 arctic aerosol and precipitation. *J. Geophys. Res*. **103**(D9), 10,975-10,990.
539 Monahan, E.C., Spiel, D.E., and Davidson, K.L. 1986. A model of marine aerosol generation
540 via whitecaps and wave disruption. In: *Oceanic Whitecaps* (edited by E. Monahan and
541 G.M. Niocaill). D. Reidel, Norwell, Mass., 167-174.
542 Mosher, B.W. 1986. The atmospheric biochemistry of selenium, PhD-Thesis. University of
543 Rhode Island, Kingston.
544 Mosher, B.W. and Duce, R.A. 1987. A global atmospheric selenium budget. *J. Geophys. Res.*
545 **92**(D11), 13,289-13,298.
546 Mosher, B.W., Duce, R.A., Prospero, J.M., Savoie, D.L. 1987. Atmospheric selenium: geo-
547 graphical distribution and ocean to atmosphere flux in the Pacific. *J. Geophys. Res.*
548 **92**(D11), 13,277-13,287.
549 Petit, J.R., Jouzel, J., Raynaud, D., Barkov, N.I., Barnola, J.-M., and co-authors. 1999. Cli-
550 mate and atmospheric history of the past 420,000 years from the Vostok ice core, Antarc-
551 tica. *Nature* **399**, 429-436.
552 Piel, C. 2004. Variabilität physikalischer und chemischer Parameter des Aerosols in der ant-
553 arktischen Troposphäre. In: *Reports on Polar and Marine Research* **476** (ed. F. Riemann).
554 Alfred-Wegener-Inst. for Polar and Marine Res., Bremerhaven.
555 Planchon, F.A.M., Boutron, C.F., Barbante, C., Cozzi, G., Gaspari, V., Wolff, E.W., Ferrari,
556 C.P., and Cescon, P. 2002. Changes in heavy metals in Antarctic snow from Coats Land
557 since the mid-19th to the late-20th century. *Earth Planet. Sci. Lett.* **200**, 207-222.

558 Rankin, A.M., Auld, V., and Wolff, E.W. 2000. Frost flowers as a source of fractionated sea
559 salt aerosol in the polar regions. *Geophys. Res. Lett.* **27**(21), 3469-3472.
560 Rankin, A.M., Wolff, E.W., and Martin, S. 2002. Frost flowers: Implications for tropospheric
561 chemistry and ice core interpretation. *J. Geophys. Res*. **107**(D23), 4683,
562 doi:10.10129/2002JD002492.
563 Reinhardt, H., Kriews, M., Miller, H., Lüdke, C., Hoffmann, E., and Skole, J. 2003. Applica-
564 tion of LA-ICP-MS in polar ice core studies. Anal. Bioanal. Chem. 375, 1265-1275,
565 doi:10.1007/s00216-003-1793-5.
566 Ruth, U., Bigler, M., Röthlisberger, R., Siggaard-Andersen, M.-L., Kipfstuhl, S., and co-
567 authors. 2007. Ice core evidence for a very tight link between North Atlantic and east
568 Asian glacial climate. *Geophys. Res. Lett.* **34** L03706, doi:10.1029/2006GL02786.
569 Smith, J., Vance, D., Kemp, R.A, Archer, C., Toms, P., King, M., Zárate, M. 2003. Isotopic
570 constraints on the source of Argentinean loess – with implications for atmospheric circula-
571 tion and the provenance of Antarctic dust during recent glacial maxima. *Earth Planet. Sci.*
572 *Lett.* **212**, 181-196.
573 Tuncel, G., Aras, N.K., and Zoller, W.H. 1989. Temporal variations and sources of elements
574 in the South Pole Aatmosphere, 1. Nonenriched and moderately enriched elements. *J.*
575 *Geophys. Res.* **94**(D10), 13,025-13,038.
576 Turner, S.M., Harvey, M.J., Law, C.S., Nightingale, P.D., and Liss, P.S. 2004. Iron-induced
577 changes in oceanic sulfur biogeochemistry. *Geophys. Res. Lett.* **31**, L14307,
578 doi:10.1029/2004GL020296.
579 Wagenbach, D. 1996. Coastal Antarctica: Atmospheric chemical composition and atmos-
580 pheric transport. In: *Chemical Exchange between the Atmosphere and polar snow* (ed.
581 E.W. Wolff and R.C. Bales). NATO ASI Series vol. **43**, Springer-Verlag Berlin Heidel-
582 berg, 173-199.

583 Wagenbach, D., Görlach, U., Moser, K., and Münnich, K.O. 1988. Coastal Antarctic aerosol:
584 the seasonal pattern of its chemical composition and radionuclide content. *Tellus* **40B**, 426-
585 436.
586 Wagenbach, D., Ducroz, F., Mulvaney, R., Keck, L., Minikin, A., Legrand, M., Hall, J.S., and
587 Wolff, E.W. 1998. Sea salt aerosol in coastal Antarctic regions. *J. Geophys. Res.* **103**(D9),
588 10 961-10 974.
589 Wedepohl, K.H. 1995. The composition of the continental crust. *Geochim. Cosmochim. Acta*
590 **59**(7), 1217-1232.
591 Wen, H. and Carignan, J. 2007. Reviews on atmospheric selenium: Emission, speciation and
592 fate. *Atmos. Environ.* **41**, 7151-7165.
593 Wolff, E.W., and Suttie E.D. 1994. Antarctic snow record of southern hemisphere lead pollu-
594 tion. *Geophys. Res. Lett.* **21**(9), 781-784.
595 Wolff, E.W., Suttie, E.D., Peel, D.A. 1999. Antarctic snow record of cadmium, copper, and
596 zinc content during the twentieth century. *Atmos. Environ.* **33**, 1535-1541.
597 Wolff, E.W., Rankin, A.M., and Röthlisberger, R. 2003. An ice core indicator of Antarctic sea
598 ice production. *Geophys. Res. Lett.* **30**(22), 2158, doi:10.1029/2003GL018454.
599 Wolff, E.W., Fischer, H., Fundel, F., Ruth, U., Twarloh, B., and co-authors. 2006. Southern
600 Ocean sea-ice extent, productivity and iron flux over the past eight glacial cycles. *Nature*
601 **440**, 491-496, doi:10.1038/nature04614.
602 Wyputta, U. (1997). On the transport of trace elements into Antarctica using measurements at
603 the Georg-von-Neumayer station. *Tellus* **49B**, 93-111.
604 Zoller, W.H., Gladney, E.S., and Duce, R.A. 1974. Atmospheric concentration of trace metals
605 at the South Pole. *Science* **183**, 198-200.

606

607 *Table 1.* Instrumental ICP-QMS detection limits (IDL, n=60) and overall method detection
608 limits (MDL, n=49) corresponding to a typical, total sampling volume of 2.0×10^4 m^3. (MDL
609 for IC-analysis given in parenthesis)
610

element	IDL	MDL
Li[pg m^{-3}]	0.12	0.21
Na[pg m^{-3}]	16	1800 (300)
Mg[pg m^{-3}]	0.44	300 (170)
K[pg m^{-3}]	32	330 (100)
Ca[pg m^{-3}]	5.0	1300 (140)
Sr[pg m^{-3}]	0.02	12
Al[pg m^{-3}]	10	220
La[pg m^{-3}]	0.005	0.07
Ce[pg m^{-3}]	0.002	0.17
Nd[pg m^{-3}]	0.006	0.09
Se[pg m^{-3}]	2.7	3.1

611

612

613

614 *Table 2.* Inter-comparison of trace elements measured by IC versus ICP-QMS: Results refer
615 to a reduced major axis regression (RMA) with slope = m, y-axis intercept = b, regression
616 coefficient = r^2.
617

Element	m	b [ng m^{-3}]	r^2
Na	1.00±0.05	24± 35	0.52
K	0.76±0.04	-0.71±1.4	0.43
Mg	1.14±0.07	-5.94±6.5	0.35
Ca	1.51±0.09	-2.05±2.1	0.42

618

Table 3. Summary of trace element composition of the aerosol measured during five years (March 1999 through December 2003) at Neumayer Station via ICP-QMS, except for Ca and K which were taken from IC-analysis. Atmospheric mean concentrations (±std) refer to standard pressure (1013 hPa) and 273.16 K.

element	overall mean	winter Apr. to Oct.	winter range	summer Nov. to Mar.	summer range
Li[pg m^{-3}]	6.1±4.1	6.9±4.5	0.2–26.5	4.9±3.1	0.17–15.0
Na[ng m^{-3}]	330±340	400±400	41-3860	220±160	0.3-820
Mg[ng m^{-3}]	52±66	62±80	6.8-760	31±22	0.17-10
K[ng m^{-3}]	16±15	17±13	0.1*-6.1	14±17	0.1*-12
Ca[ng m^{-3}]	15±15	19±17	0.14*-67	11±8.6	0.14*-26.4
Al[ng m^{-3}]	1.0±0.7	0.84±0.6	0.22*-3.2	1.3±0.7	0.23-3.7
Sr[ng m^{-3}]	0.29±0.27	0.36±0.31	0.012*-2.6	0.19±0.13	0.012*-0.53
La[pg m^{-3}]	0.86±0.7	0.56±0.5	0.07*-3.1	1.32±0.8	0.07*-5.8
Ce[pg m^{-3}]	1.6±1.3	1.0±0.8	0.17*-5.5	2.5±1. 5	0.17*-10.5
Nd[pg m^{-3}]	0.7±0.6	0.47±0.45	0.09*-2.7	1.1±0.6	0.09*-4.4
Se[pg m^{-3}]	19±18	16±11	3.1*-82	25±24	3.1*-160

* method detection limit (MDL)

627

628 *Table 4.* Al, La, Na, and Se concentrations (±std) measured in Antarctic aerosol samples.

629

element	winter	summer	sampling period	site[a]
Al	-	570±170	10/1970	SP (Zoller et al., 1974)
[pg m^{-3}]	300±40	830±410	1971/75/76/78	SP (Cunningham & Zoller, 1981)
	320±110	730±240	2/1979 – 11/1983	SP (Tuncel et al., 1989)
	-	194±19	12/1984 – 02/1985	AP (Dick, 1991)
	9470[b]	13290[b]	1985-1988	AP (Artaxo et al., 1992)
	840±600	1270±700	3/1999 – 12/2003	NM, this study
La	-	0.51±0.37	10/1970	SP (Zoller et al., 1974)
[pg m^{-3}]	< 2	0.78±0.25	1971/75/76/78	SP (Cunningham & Zoller, 1981)
	0.43±0.11	0.56±0.21	2/1979 – 11/1983	SP (Tuncel et al., 1989)
	0.56±0.5	1.32±0.8	3/1999 – 12/2003	NM, this study
Na	-	7.2±3.8	10/1970	SP (Zoller et al., 1974)
[ng m^{-3}]	40±31	5.1±1.7	1971/75/76/78	SP (Cunningham & Zoller, 1981)
	31±14	8.7±3.2	2/1979 – 11/1983	SP (Tuncel et al., 1989)
	869.9[b]	1046.2[b]	1985-1988	AP (Artaxo et al., 1992)
	-	27.6±0.4	12/1984 – 02/1985	AP (Dick, 1991)
	400±400	220±160	3/1999 – 12/2003	NM, this study
Se	-	5.6±1.2	10/1970	SP (Zoller et al., 1974)
[pg m^{-3}]	6.9±2.7	6.3±6	1971/75/76/78	SP (Cunningham & Zoller, 1981)
	4.8±0.8	8.4±1.6	2/1979 – 11/1983	SP (Tuncel et al., 1989)
	118[b]	122[b]	1/1983 – 12/1984	AP (Artaxo et al., 1992)
	16±11	25±24	3/1999 – 12/2003	NM, this study

630 [a]AP = Antarctic Peninsula, SP = South Pole, NM = Neumayer
631 [b]sum of fine and coarse mode
632

FIGURES

Fig. 1: (a) Mean element enrichment factors with respect to earth crust (EF_{crust}) and (b) sea salt composition (EF_{ss}) of Neumayer aerosol samples dissected for summer (November through March) and winter (April through October), respectively.

Fig. 2: Atmospheric Na, Li, and Sr concentrations measured at Neumayer Station at weekly time resolution. The grey bars mark the method detection limits.

Fig. 3: Same as Figure 2 but for Al, La, Ce, and Nd.

Fig. 4: Pie diagram of the aerosol composition (weight percent referring to the sum of the measured species) at Neumayer during winter and summer, respectively.

Fig. 5: Mean annual cycle of major mass fractions in Neumayer aerosol samples: Sea salt (circles), biogenic sulfur (i.e. the sum of MS and nss-SO_4^{2-}, drawn line), and mineral dust (diamonds) portion.

Fig. 6: Seasonality of monthly concentration mean of sea salt (Na) and mineral dust (La) reference elements. Values correspond to 5 years of observation (i.e. about 20 samples per month). Error bars indicate the respective standard deviation.

Fig. 7: Time series of wind velocity at Neumayer during the sampling period displayed in the same temporal resolution as filter sampling (seven days, thin line), and 6 points moving average (bold grey line).

659

660 *Fig. 8:* Notched box plots for enrichment factors respecting standard mean ocean water com-
661 position for the sea salt portion of Li, K, Mg, Ca, and Sr. Lines in the middle of the boxes
662 represent sample medians (values are given aside), lower and upper lines of the boxes are the
663 25^{th} and 75^{th} percentiles, whiskers show the range of the sample values while outliers are
664 marked by "+" signs. The widths of the notches indicate the confidence interval of the me-
665 dian.

666

667 *Fig. 9:* Double-logarithmic plot of ssLi, ssMg, and ssSr vs. ssNa. Bold grey lines represent
668 the relation for standard mean ocean water.

669

670 *Fig. 10:* Time series of Se and MS (shifted y-axis) concentrations measured at Neumayer.
671 The grey bar marks the method detection limit for Se.

672

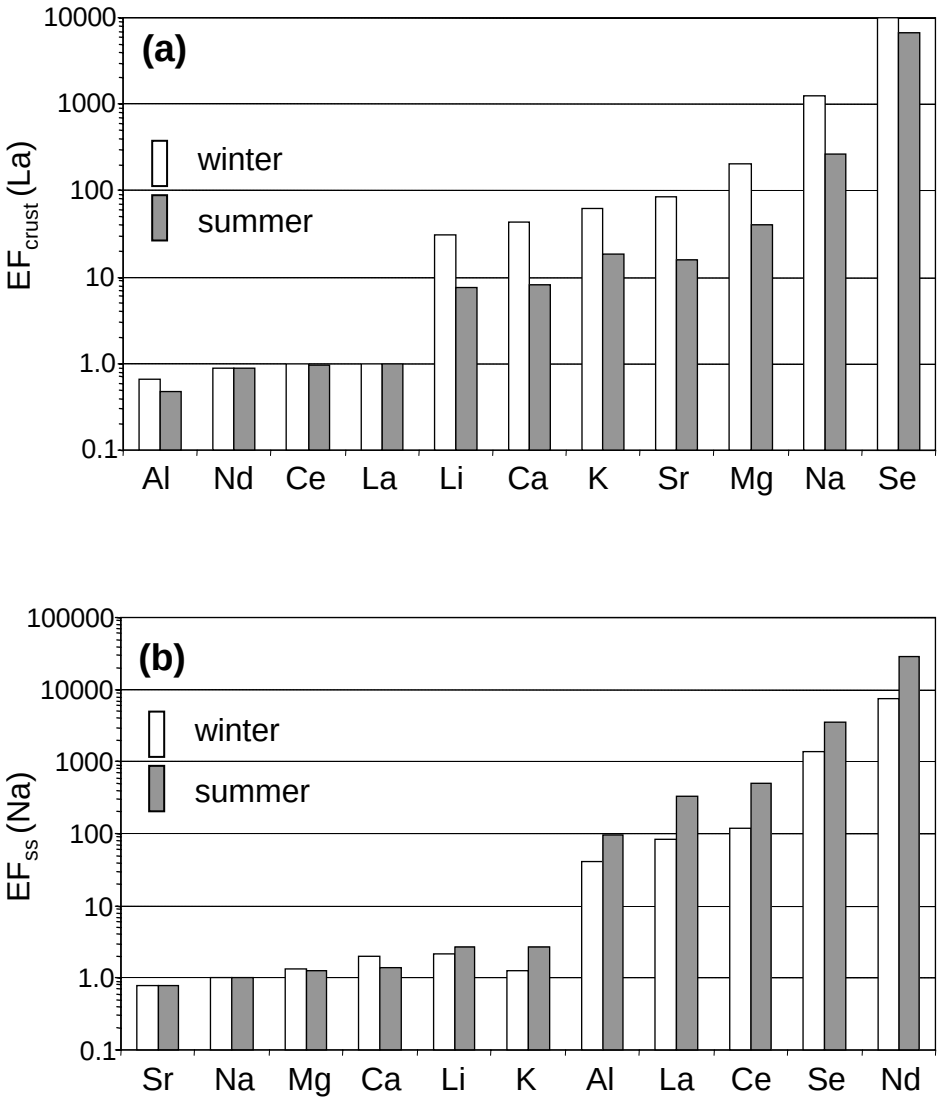

Figure 1: (a) Mean element enrichment factors with respect to earth crust (EF_{crust}) and (b) sea salt composition (EF_{ss}) of Neumayer aerosol samples dissected for summer (November through March) and winter (April through October), respectively.

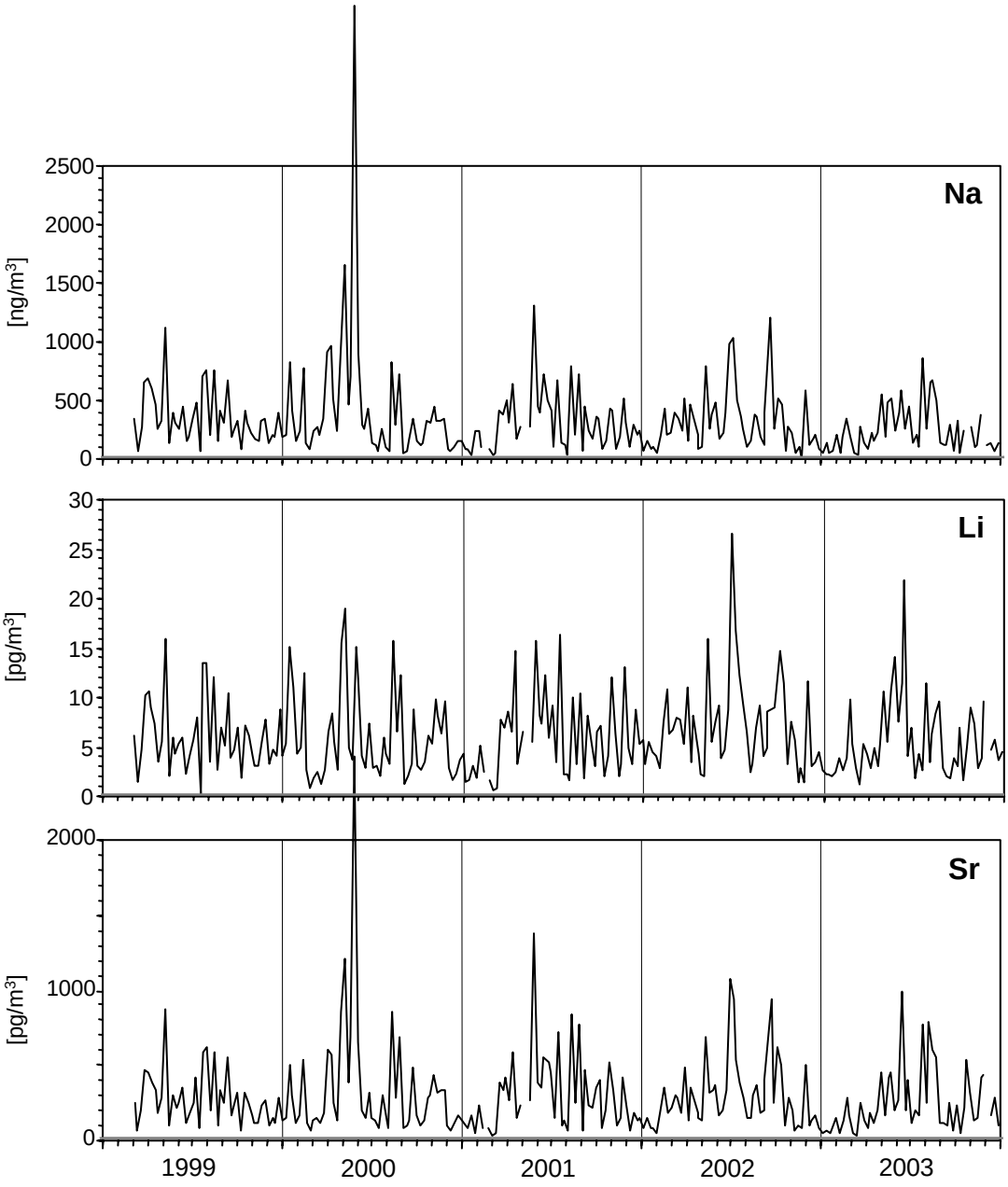

Figure 2: Atmospheric Na, Li, and Sr concentrations measured at Neumayer Station at weekly time resolution. The grey bars mark the method detection limits.

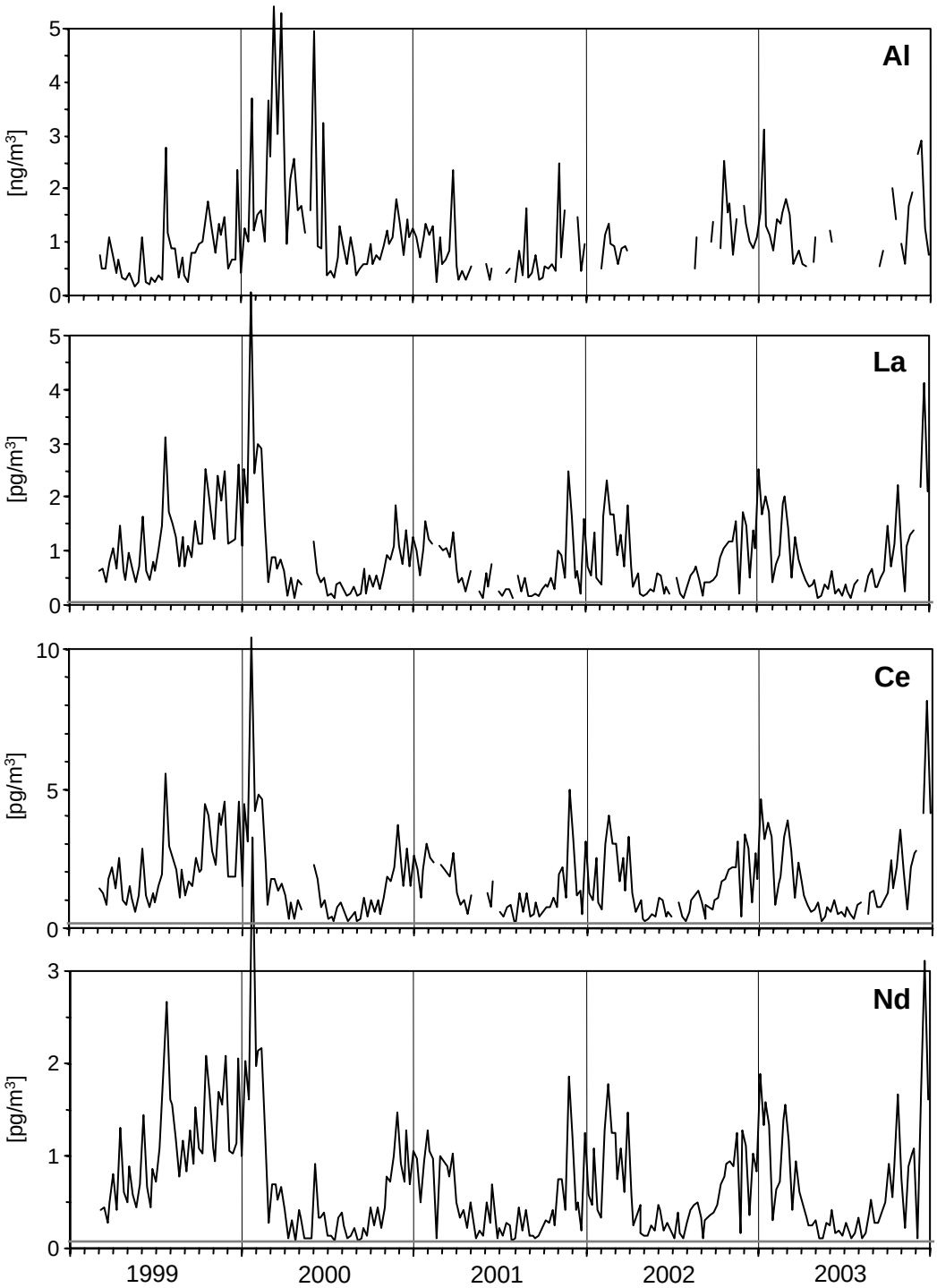

Figure 3: Same as Figure 2 but for Al, La, Ce, and Nd.

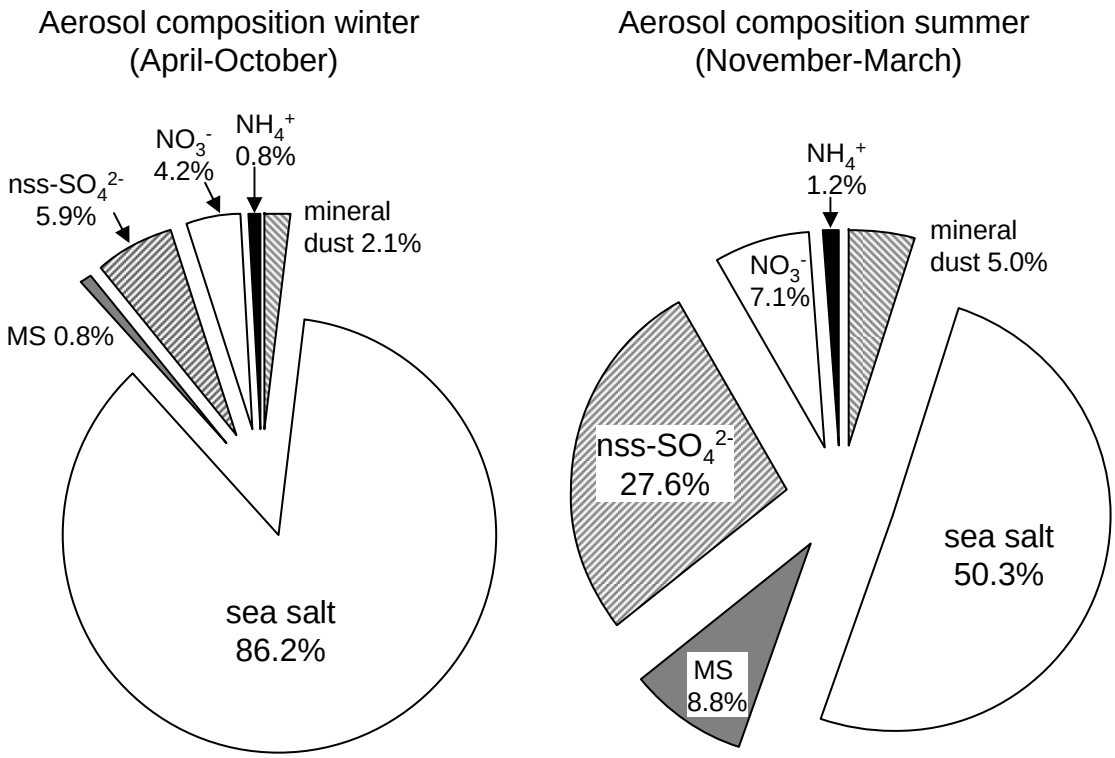

Figure 4: Pie diagram of the aerosol composition (weight percent referring to the sum of the measured species) at Neumayer during winter and summer, respectively.

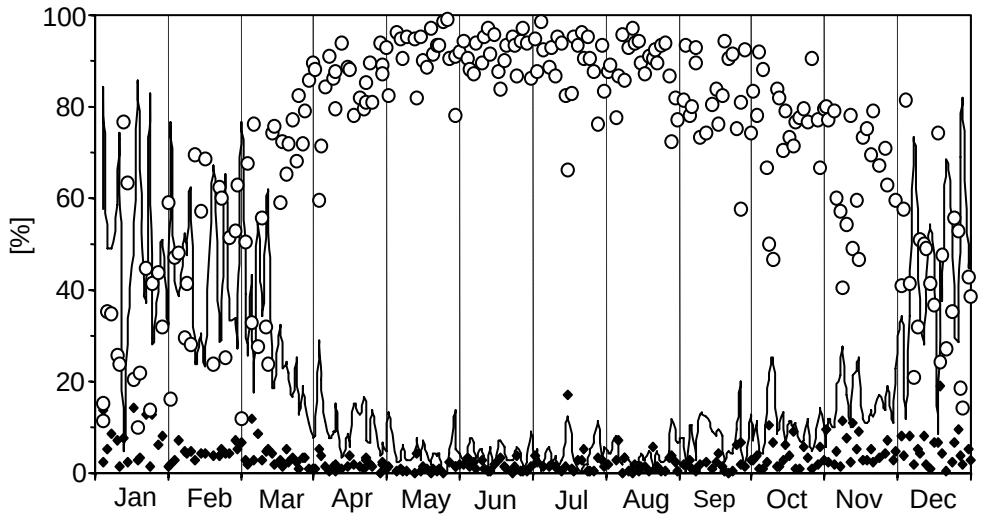

Figure 5: Mean annual cycle of major mass fractions in Neumayer aerosol samples: Sea salt (circles), biogenic sulfur (i.e. the sum of MS and nss-SO_4^{2-}, drawn line), and mineral dust (diamonds) portion.

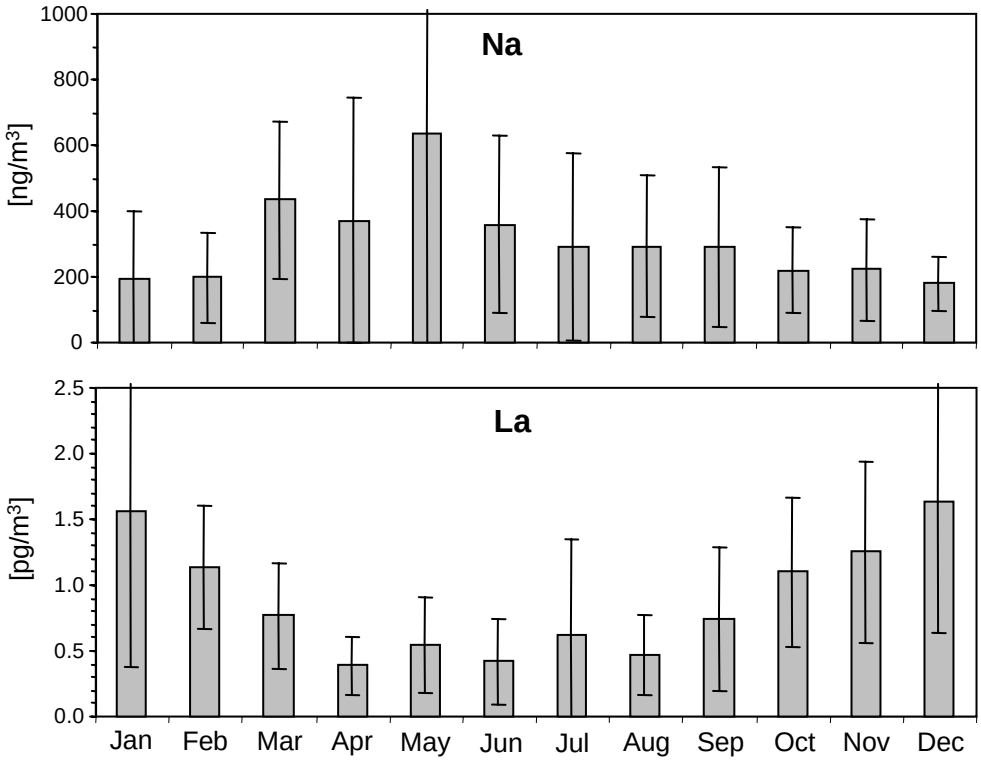

Figure 6: Seasonality of monthly concentration means of sea salt (Na) and mineral dust (La) reference elements. Values correspond to 5 years of observation (i.e. about 20 samples per month). Error bars indicate the respective standard deviation.

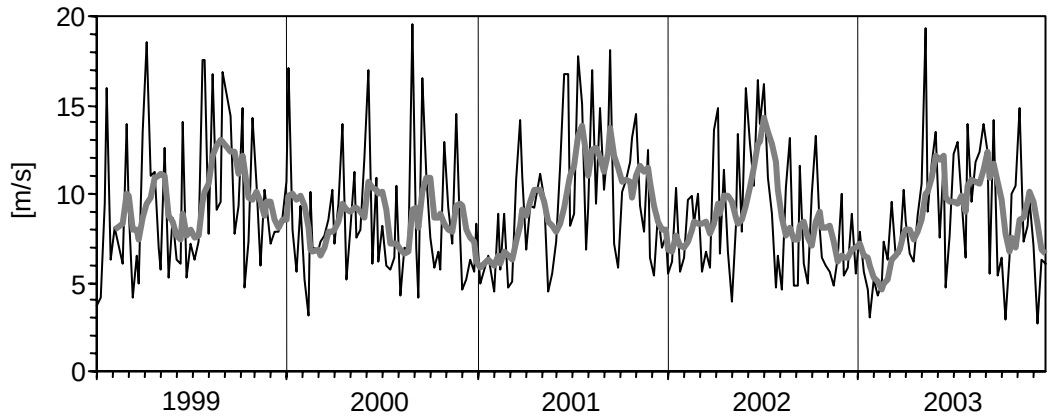

Figure 7: Time series of wind velocity at Neumayer during the sampling period displayed in the same temporal resolution as filter sampling (seven days, thin line), and 6 points moving average (bold grey line).

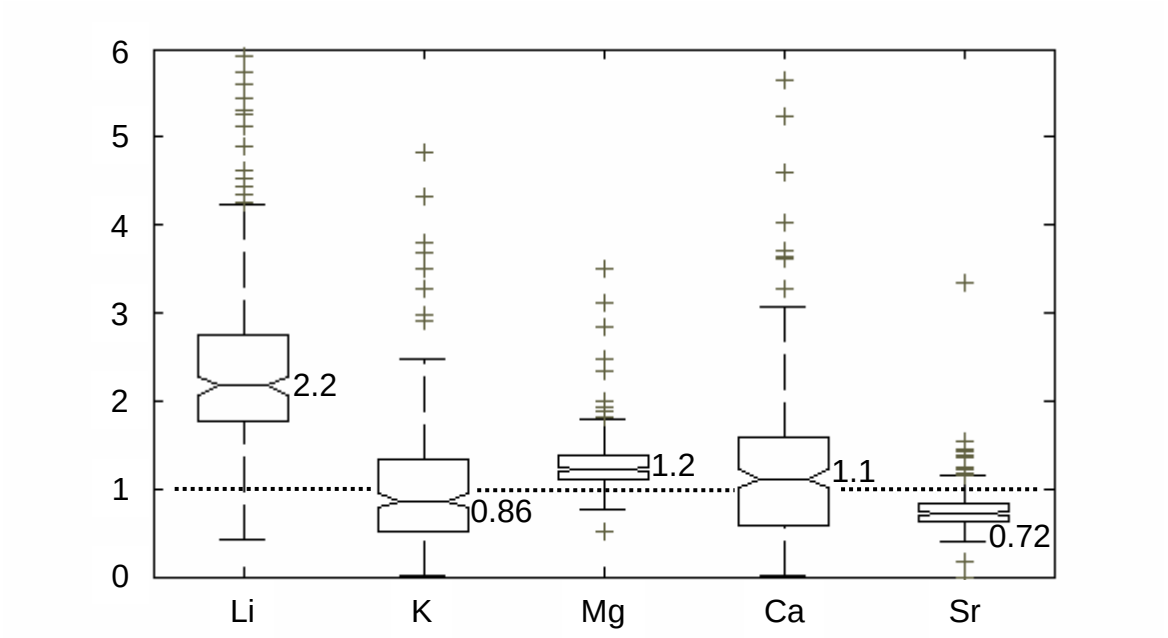

Figure 8: Notched box plots for enrichment factors respecting standard mean ocean water composition for the sea salt portion of Li, K, Mg, Ca, and Sr. Lines in the middle of the boxes represent sample medians (values are given aside), lower and upper lines of the boxes are the 25^{th} and 75^{th} percentiles, whiskers show the range of the sample values while outliers are marked by "+" signs. The widths of the notches indicate the confidence interval of the median.

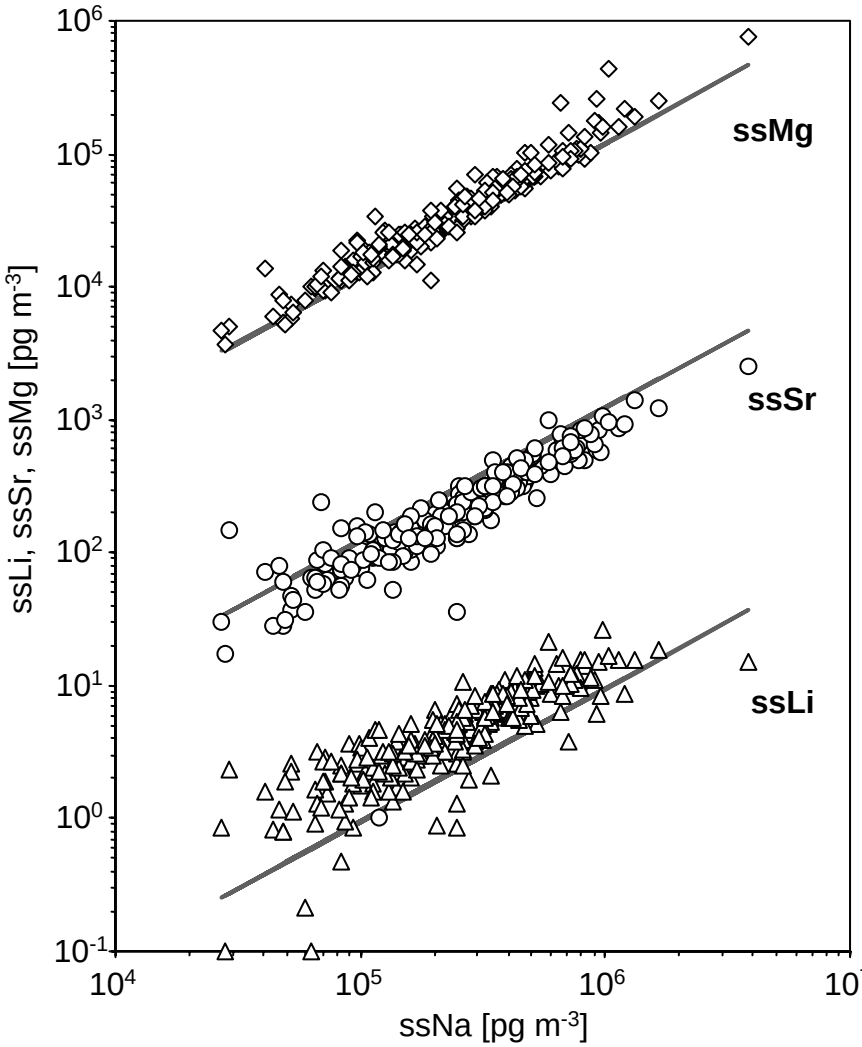

Figure 9: Double-logarithmic plot of ssLi, ssMg, and ssSr vs. ssNa. Bold grey lines represent the relation for standard mean ocean water.

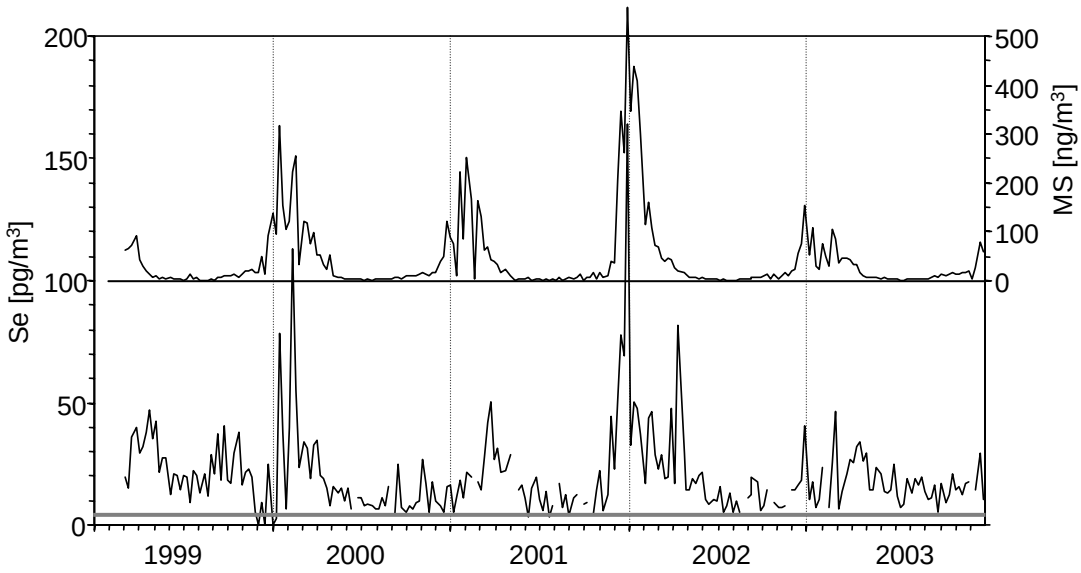

Figure 10: Time series of Se and MS (shifted y-axis) concentrations measured at Neumayer. The grey bar marks the MDL for Se.